

Published in final edited form as:

JAMA Neurol. 2014 January ; 71(1): 11–22. doi:10.1001/jamaneurol.2013.4544.

Brain Differences in Infants at Differential Genetic Risk for Late-Onset Alzheimer Disease:

A Cross-sectional Imaging Study

Douglas C. Dean III, MSc, Beth A. Jerskey, PhD, Kewei Chen, PhD, Hillary Protas, PhD, Pradeep Thiyyagura, MS, Auttawat Roontiva, MS, Jonathan O’Muircheartaigh, PhD, Holly Dirks, BSc, Nicole Waskiewicz, BSc, Katie Lehman, BSc, Ashley L. Siniard, PhD, Mari N. Turk, PhD, Xue Hua, PhD, Sarah K. Madsen, BS, Paul M. Thompson, PhD, Adam S. Fleisher, MD, Matthew J. Huentelman, PhD, Sean C. L. Deoni, PhD, and Eric M. Reiman, MD
Advanced Baby Imaging Lab, School of Engineering, Brown University, Providence, Rhode Island (Dean, O’Muircheartaigh, Dirks, Waskiewicz, Lehman, Deoni); Alpert Medical School of Brown University, Providence, Rhode Island (Jerskey); Banner Alzheimer’s Institute, Phoenix, Arizona (Chen, Protas, Thiyyagura, Roontiva, Fleisher, Reiman); Department of Mathematics, Arizona State University, Tempe (Chen); Department of Radiology, University of Arizona School of Medicine, Tucson (Chen); Arizona Alzheimer’s Consortium, Phoenix (Chen, Protas, Thiyyagura, Roontiva, Siniard, Fleisher, Huentelman, Reiman); Department of Neuroimaging, King’s College London, Institute of Psychiatry, London, England (O’Muircheartaigh); Department of Neurology, University of California, San Diego School of Medicine, San Diego (Fleisher); Neurogenomics Division, Translational Genomics Research Institute, Phoenix, Arizona (Siniard, Turk, Huentelman, Reiman); Imaging Genetics Center, Laboratory of Neuro Imaging, Department of Neurology, University of California, Los Angeles School of Medicine, Los Angeles (Hua, Madsen, Thompson); Department of Psychiatry, University of Arizona School of Medicine, Phoenix (Reiman).

Abstract

IMPORTANCE—Converging evidence suggests brain structure alterations may precede overt cognitive impairment in Alzheimer disease by several decades. Early detection of these alterations holds inherent value for the development and evaluation of preventive treatment therapies.

Copyright 2014 American Medical Association. All rights reserved.

Corresponding Author: Sean C. L. Deoni, PhD, Advanced Baby Imaging Lab, School of Engineering, Brown University, Providence, RI 02912 (sdeoni@mac.com).

Author Contributions: Dr Deoni had access to all of the data in the study and takes responsibility for the integrity of the data and the accuracy of the data analysis. Mr Dean and Drs Jerskey and Chen are shared first authors. Drs Deoni and Reiman are shared senior authors. *Study concept and design:* Dean, Jerskey, Thompson, Fleisher, Deoni, Reiman. *Acquisition of data:* Dean, Jerskey, Dirks, Waskiewicz, Lehman, Siniard, Turk, Huentelman, Deoni, Reiman. *Analysis and interpretation of data:* Dean, Chen, Protas, Thiyyagura, Roontiva, O’Muircheartaigh, Siniard, Turk, Hua, Madsen, Thompson, Fleisher, Huentelman, Deoni, Reiman. *Drafting of the manuscript:* Dean, Jerskey, Dirks, Hua, Deoni. Critical revision of the manuscript for important intellectual content: Dean, Chen, Protas, Thiyyagura, Roontiva, O’Muircheartaigh, Waskiewicz, Lehman, Siniard, Turk, Madsen, Thompson, Fleisher, Huentelman, Deoni, Reiman. *Statistical analysis:* Dean, Chen, Protas, Thiyyagura, Roontiva, O’Muircheartaigh, Hua, Deoni, Reiman. *Obtained funding:* Huentelman, Deoni, Reiman. *Administrative, technical, or material support:* Dean, Jerskey, Dirks, Waskiewicz, Lehman, Huentelman, Deoni, Reiman. *Study supervision:* Chen, Thompson, Huentelman, Deoni, Reiman.

Conflict of Interest Disclosures: None reported.

OBJECTIVE—To compare magnetic resonance imaging measurements of white matter myelin water fraction (MWF) and gray matter volume (GMV) in healthy infant carriers and noncarriers of the apolipoprotein E (*APOE*) ϵ 4 allele, the major susceptibility gene for late-onset AD.

DESIGN, SETTING, AND PARTICIPANTS—Quiet magnetic resonance imaging was performed at an academic research imaging center on 162 healthy, typically developing 2- to 25-month-old infants with no family history of Alzheimer disease or other neurological or psychiatric disorders. Cross-sectional measurements were compared in the *APOE* ϵ 4 carrier and noncarrier groups. White matter MWF was compared in one hundred sixty-two 2- to 25-month-old sleeping infants (60 ϵ 4 carriers and 102 noncarriers). Gray matter volume was compared in a subset of fifty-nine 6- to 25-month-old infants (23 ϵ 4 carriers and 36 noncarriers), who remained asleep during the scanning session. The carrier and noncarrier groups were matched for age, gestational duration, birth weight, sex ratio, maternal age, education, and socioeconomic status.

MAIN OUTCOMES AND MEASURES—Automated algorithms compared regional white matter MWF and GMV in the carrier and noncarrier groups and characterized their associations with age.

RESULTS—Infant ϵ 4 carriers had lower MWF and GMV measurements than noncarriers in precuneus, posterior/middle cingulate, lateral temporal, and medial occipitotemporal regions, areas preferentially affected by AD, and greater MWF and GMV measurements in extensive frontal regions and measurements were also significant in the subset of 2- to 6-month-old infants (MWF differences, $P < .05$, after correction for multiple comparisons; GMV differences, $P < .001$, uncorrected for multiple comparisons). Infant ϵ 4 carriers also exhibited an attenuated relationship between MWF and age in posterior white matter regions.

CONCLUSIONS AND RELEVANCE—While our findings should be considered preliminary, this study demonstrates some of the earliest brain changes associated with the genetic predisposition to AD. It raises new questions about the role of *APOE* in normal human brain development, the extent to which these processes are related to subsequent AD pathology, and whether they could be targeted by AD prevention therapies.

What are the earliest brain changes associated with the predisposition to Alzheimer disease (AD)? The amyloid cascade hypothesis suggests that AD begins with accumulation of β -amyloid 1-42 ($A\beta$ 1-42) proteins into oligomeric and fibrillar assemblies, leading to neuroinflammatory changes, accumulation, propagation and phosphorylation of the microtubule-associated protein tau, and dysfunction and loss of synapses and neurons.^{1,2} While cerebral $A\beta$ deposition may begin 1 to 2 decades prior to the onset of cognitive impairment,³⁻⁵ recent studies suggest functional and structural brain alterations may precede the onset of $A\beta$ deposition in carriers of the apolipoprotein E (*APOE*) ϵ 4 allele, the major late-onset AD susceptibility gene, and in carriers of a rare early-onset autosomal dominant AD mutation.⁶⁻¹⁰ These findings have led us to explore even earlier brain differences in individuals at differential genetic risk of AD.

The *APOE* ϵ 4 allele is found in about one-quarter of the population and about 60% of patients with AD dementia.¹¹ Each additional copy of the ϵ 4 allele in a person's *APOE* genotype is associated with a heightened risk of AD and an earlier average age at dementia onset.^{12,13} In a positron emission tomography study, we have previously shown that young

adult *APOE* $\epsilon 4$ carriers have lower cerebral metabolic rates of glucose than noncarriers in brain regions preferentially affected by AD, almost 5 decades before their average age at possible dementia onset.⁷ While carriers did not have greater age-related cerebral metabolic rates of glucose decline than noncarriers between young adulthood and late middle age, the metabolic reductions were located in regions preferentially and progressively affected by metabolic decline and amyloid deposition in the later preclinical and clinical stages of AD. In a subsequent postmortem study, we and our colleagues found that young adult *APOE* $\epsilon 4$ carriers had less cytochrome-*c* oxidase activity (a measure of oxidative metabolism) in brain tissue from the posterior cingulate (one of the regions preferentially affected by AD), even in the absence of soluble or fibrillar A β .⁹

These findings, as well as those from other structural, functional, and functional connectivity magnetic resonance imaging (MRI) studies of older children and young adults at differential genetic risk for AD,¹⁴⁻¹⁶ led us to postulate that *APOE* $\epsilon 4$ carriers have neurodevelopmental alterations that provide a foothold for the neuropathological changes associated with the subsequent course of AD. Indeed, researchers recently used volumetric MRI to explore differences in regional gray matter volume (GMV) in 1- to 3-month-old carriers and noncarriers of the *APOE* $\epsilon 4$ allele (as well as in carriers and noncarriers of 4 other genes implicated in the predisposition to several psychiatric disorders) who were enriched for a reported parental history of psychiatric disorders and use of psychotropic medications.¹⁷ Additional studies are needed to extend *APOE* $\epsilon 4$ -related GMV findings to healthy infants without a parental history of psychiatric or neurological disorders or medication use, include other brain imaging measurements and infants from a broader age range, and clarify the extent to which these measurements change during the course of brain development.

In this cross-sectional brain imaging study, we sought to characterize and compare regional GMV and a white matter myelin content measure in healthy infant $\epsilon 4$ carriers and noncarriers 2 to 25 months of age. To do so, we used unusually quiet MRI techniques that were developed specifically for the study of naturally sleeping infants and toddlers.¹⁷ A T1-weighted volumetric MRI scan was used to assess regional GMV. An imaging technique called mcDESPOT¹⁸ (multi-component Driven Equilibrium Single Pulse Observation of T1 and T2) was used to assess regional myelin water fraction (MWF), a quantitative measure sensitive to myelin that we have previously used to investigate infant brain development^{18,19} and demyelinating disorders such as multiple sclerosis.^{20,21} Prior mcDESPOT investigations of white matter development throughout infancy and early childhood have mirrored the histologically established spatiotemporal pattern of myelination,²² and histological comparisons in a dysmyelinating “shaking-pup” model²³ have demonstrated the method’s sensitivity and specificity to detect myelin. Automated voxel-based image-analysis algorithms were used to compare regional MWF and GMV to characterize and compare age-related trajectories in the 2- to 25-month-old $\epsilon 4$ carrier and noncarrier groups.

Methods

Study Design and Participants

Data from 162 healthy, typically developing, 2- to 25-month-old infants were included in this study. All participants and families were recruited from the local area via pamphlets and

flyers at community events, parks, day care centers, play centers, etc. To help mitigate potential confounds beyond *APOE* genotype, rigorous selection criteria included the following: healthy singleton birth between 37 and 42 weeks' gestation; APGAR score of at least 8; no abnormalities on fetal ultrasonography; no reported history of neurological events or disorders in the infant (ie, head trauma, ischemia, or epilepsy, for example); no admissions to the neonatal intensive care unit; no family history of a psychiatric or neurological disorder in the infants' parents or siblings; no complications (ie, pre-eclampsia) during pregnancy; and no reports of illicit drug or alcohol use during pregnancy. These criteria were confirmed during parental interviews at the time of enrollment. Extensive infant, parent, and sibling medical and family history questionnaires were also used to provide information about the prospective infants' neurological, psychiatric, and other medical events and disorders; maternal and paternal education levels; maternal prenatal and postnatal health, substance use, and breastfeeding practices; gestation duration; and birth weight. Written informed consent was obtained from each infant's parents or legal guardian, and the study was performed under guidelines approved by the Brown University institutional review board. Parents were not informed of their child's *APOE* genotype, in accordance with the informed consent and institution's institutional review board policies.

Data were used as follows to characterize and compare regional MWF and GMVs in infant $\epsilon 4$ carrier and noncarrier groups. (1) The MWF images from one hundred sixty-two 2- to 25-month-old infants were used to compare regional myelin content in 60 $\epsilon 4$ carriers and 102 noncarriers. The MWF images from the thirty-six 2- to 6-month-old infants were subsequently used to compare regional white matter content in the 14 $\epsilon 4$ carriers and 22 noncarriers and confirm the implicated MWF findings at even younger ages. (2) T1-weighted volumetric images from 59 of the 6- to 22-month-old infants were used to compare regional GMV in 23 $\epsilon 4$ carriers and 36 noncarriers. (As noted in the Results section, T1-weighted MRIs were not available in eighty-one 6- to 25-month-old infants since they awakened prior to the completion of the scan. The MRIs from the 22 infants younger than 6 months were excluded from the GMV analysis because of an inability of the automated algorithm to generate adequate segmented gray matter images in 5 of the 7 $\epsilon 4$ carriers and 4 of the 15 $\epsilon 4$ noncarriers, as discussed later.) (3) The MWF images from the one hundred sixty-two 2- to 25-month-old infants and T1-weighted images from the fifty-nine 6- to 22-month-old infants were used to explore associations between age and brain imaging measurements in the $\epsilon 4$ carrier and noncarrier groups.

MRI Methods

All imaging was performed between July 2010 and October 2012 at the Brown University MRI facility on a Siemens Tim Trio 3-T scanner equipped with a 12-channel head RF array. Imaging was performed at night during natural nonsedated sleep to minimize infant motion during acquisition. To reduce the likelihood of the child awaking during the scan, imaging times were kept under 40 minutes. Scanner noise levels were lessened by slowing the gradient switching rate and reducing the maximum gradient amplitudes to 15 mT/m/s and 30 mT/m, respectively. Further acoustic attenuation was achieved through a sound-attenuating bore insert (Ultra Barrier HD Composite; UltraBarrier USA) and electrodynamic headphones that played white noise throughout the acquisition. Estimated noise levels were

less than 65 dB. Appropriately sized pediatric MedVac vacuum immobilization bags (CFI Medical Solutions) and foam cushions were used to cradle the infant and limit intrascan motion. While the reduced scanning speed minimizes acquisition noise, it does result in longer scans, which increases the possibility of motion artifacts or missing data due to the child awaking during the scan. In all data acquired for this study, infants and toddlers remained asleep throughout the entirety of the scan and motion, measured through the intrascan registration step (see later), was less than 1 mm across the entire experiment.

The MWF data related to white matter microstructure and sensitive to changes in myelin content were acquired using mcDESPOT imaging protocols optimized for infants and young toddlers.¹⁸ These protocols involve acquiring 8 T1-weighted spoiled gradient recalled echo images (SPGR) (spoiled fast low-angle shot), 2 inversion-prepared (IR)-SPGR images, and 16 T1/T2-weighted steady-state free precession (SSFP) (true fast imaging with steady-state precession) images. As stated, mcDESPOT has been used previously to investigate normative white matter development in healthy infants and young children.^{18,19} A higher resolution T1-weighted IR-SPGR volumetric scan was subsequently acquired in those infants who remained asleep, providing measures of regional GMV. All imaging data were visually inspected to ensure they were free of motion or other corrupting artifacts (such as blurring, ghosting, or ringing).

As a brief overview, mcDESPOT is a rapid multicomponent relaxometry technique that interrogates tissue microstructure by decomposing the measured MRI signal into contributions from distinct microanatomical water pools. In brain parenchyma, water is broadly categorized as residing in the less-restricted intracellular and extracellular water, within the tightly bound water trapped between the lipid bilayers of the myelin sheath, or within the unrestricted cerebral spinal fluid.²⁴ Based on the differing biophysical properties of these environments, they each exhibit differing T1 and T2 relaxation properties. Through the acquisition of multiple T1- and T2-weighted images, and the fitting of appropriate multicomponent tissue models (eg, Figure 1), mcDESPOT aims to estimate each water pool's relaxation properties and relative volume fraction.²⁵ The myelin volume fraction, MWF, is the relative fraction of water within the myelin sheath and has been shown to correlate well with histological estimates of myelin content and has been used extensively in the study of multiple sclerosis.^{26,27} In addition to multiple sclerosis,^{20,21} and amyotrophic and primary lateral sclerosis,²⁸ mcDESPOT has been used to investigate normative white matter development in healthy infants and young children.^{18,19}

Following successful scanning, buccal swab samples were obtained from each infant, DNA was isolated, and *APOE* genotypes were characterized.

Image Analysis

Regional MWF Comparisons—The MWF maps were calculated for each of the 162 infants and coregistered to a common template using the Advanced Normalization Tools software package.²⁸ To derive the MWF measures, the individual SPGR, IR-SPGR, and balanced SSFP images were first linearly coregistered to account for subtle intrascan head motion,²⁹ and nonparenchyma signal was removed from each image using an automated deformable model approach.³⁰ The IR-SPGR images were used in conjunction with the

SPGR images to correct for transmit (B_1) magnetic field inhomogeneities, while main magnetic field inhomogeneities were corrected by acquiring the balanced SSFP data with 2 phase-cycling schemes.³¹ The MWF maps were then derived by fitting the SPGR and balanced SSFP images to a 3-pool, multicomponent relaxation model.²⁵

To align each infant's mcDESPOT MWF map to a common analysis space, the high-flip angle SPGR image was first nonlinearly registered to an age-specific template. Using this nonlinear transformation as well as previously calculated transformations¹⁸ from the age-specific templates to a higher-level template (that had been rigidly coregistered to the Montreal Neurological Institute T1-weighted template), the quantitative MWF maps were transformed into the space of the study template.

Regional MWF comparisons were performed using the full cohort of 2- to 25-month-old infants to characterize early developmental differences between carriers and noncarriers. To identify the earliest changes, this analysis was repeated using a subset of thirty-six 2- to 6-month-old infants. Data were smoothed with a modest 2.5-mm full-width-at-half-maximum gaussian kernel and the voxelwise unpaired t tests were performed via nonparametric permutation testing using the Randomize module of the FMRIB Software Library (<http://fsl.fmrib.ox.ac.uk/fsl/fslwiki/>). We chose 2.5-mm smoothing based on the relative size of the infant and toddler head, as well as to maintain the fidelity of the underlying imaging data.

Significance was defined as $P < .05$ corrected for multiple comparisons using a cluster-based technique, a commonly used multiple testing method for determining corrected significances while accounting for the high level of spatial dependencies between adjacent voxels.³² Contiguous clusters were first identified using a threshold of $P < .005$ ($t > 3.1$). For visualization purposes, the statistical brain maps were superimposed sections from the spatial standardized volume-rendered brain MRI of a healthy 12-month-old infant (Figure 2).

Regional GMV Comparison—For the 6- to 22-month-old infants with high-resolution volumetric T1-weighted MRIs, the VBM8 toolbox in the SPM8 brain-mapping platform³³ was used to generate segmented gray matter images, deform each image to the coordinates of a standardized brain atlas using an infant MRI template (to which the quality of the gray matter segmentation was semiquantitatively checked), smooth the spatially normalized gray matter maps with an 8-mm full-width-at-half-maximum gaussian kernel, and use a voxelwise general linear model to characterize between-group difference in regional GMV between the 23 ε4 carriers and 36 noncarriers ($P < .001$, uncorrected for multiple comparisons). The false discovery rate subroutine was used to assess significance after correction for multiple regional comparisons. For visualization purposes, the statistical brain map was superimposed onto the spatial standardized volume-rendered brain MRI of a healthy 12-month-old infant (Figure 3). As previously noted, T1-weighted MRIs from the twenty-two 2- to 6-month-old infants were excluded from the GMV analysis because of an inability of the automated algorithm to generate adequate segmented gray matter images in 9 of these infants.

Associations Between Brain Imaging Measurements and Age

In subsequent analyses, we characterized and compared relationships between brain imaging measures and age in the $\epsilon 4$ carrier and noncarrier groups (Figure 4). Logarithmic developmental trajectories ($MWF[age] = A \times \log[age] - B$) were used to characterize and compare associations between regional MWF and age in each group (A). A bootstrap fitting approach with residual resampling³⁴ was used to fit 750 curves in each group at each image voxel, and the resulting trajectory distributions were compared using an unpaired t test with cluster-based correction for multiple comparisons as described earlier. To explore associations between regional GMV and age, individual infant measurements were extracted from the precuneus, precuneus/cingulate, lateral temporal, medial occipitotemporal, and frontal atlas locations in Table 1 that were associated with maximally significant between-group differences in regional GMV. These data were used to perform linear regressions between regional GMV and age and to characterize and compare linear slopes in the $\epsilon 4$ carrier and noncarrier groups. While the analysis of age-related MWF change used a logarithmic trajectory, a linear trajectory model was used to confirm the logarithmic findings and compare the 2 fits. We also confirmed our bootstrap analysis by examining the voxelwise $\log(\text{age}) \times \epsilon 3/\epsilon 4$ group interaction.

Results

Groups

As previously noted, MWF images from 162 infants, 2 to 25 months of age, including 60 $\epsilon 4$ carriers and 102 noncarriers, were used to assess regional white matter myelin content. T1-weighted volumetric images from 59 of the infants, 6 to 22 months of age, including 23 $\epsilon 4$ carriers and 36 noncarriers, were used to assess regional GMV. T1-weighted volumetric images were not available in 81 of the other 6- to 25-month-old infants, including 30 $\epsilon 4$ carriers and 51 noncarriers who awakened prior to completion of the latter scan. (There were no significant differences between the proportions of $\epsilon 4$ carriers and noncarriers in the 6- to 25-month-old groups with and without available T1-weighted volumetric images.)

Contrast between gray and white matter was insufficient to generate adequate segmented gray matter images in 9 of the 22 infants younger than 6 months, including 5 of the 7 $\epsilon 4$ carriers and 4 of the 15 noncarriers during the automated image-analysis algorithm's initial preprocessing stage. For this reason, T1-weighted MRIs from all 22 of the infants younger than 6 months were excluded from the GMV analysis to eliminate the potential for differential selection bias in the youngest infant carrier and noncarrier groups. The fact that insufficient contrast between gray matter and white matter was observed only in some of the youngest infants and in a higher proportion of $\epsilon 4$ carriers than noncarriers ($\chi^2, P = .047$) could reflect less myelin content in the youngest infant age range, particularly in the carrier group. This possibility is supported by the mcDESPOT-generated MWF findings given later.

Characteristics and additional demographic features of the infant $\epsilon 4$ carrier and noncarrier groups in each comparison are shown in Table 2 and Table 3. Infant *APOE* $\epsilon 4$ carrier and noncarrier groups in the respective 2- to 25-month-old MWF, 2- to 6-month-old MWF, and

6- to 22-month-old GMV comparisons did not differ significantly in their age (corrected for 40-week gestation), birth weight, maternal age, socioeconomic status, educational level, male-female ratio, breastfed to bottle-fed ratio, reported in utero alcohol exposure, vaginal to cesarean birth ratio, or parental marital status.

2- to 25-Month-Old and 2- to 6-Month-Old MWF Comparisons

Differences between the infant *APOE* $\epsilon 4$ carrier and noncarrier groups in regional MWF, including those in the entire 2- to 25-month-old cohort and those in the 2- to 6-month-old subset, are shown in Figure 2 and Table 1. Compared with noncarriers, the 2- to 25-month-old $\epsilon 4$ carriers had significantly lower MWF in posterior white matter regions, including the optic radiations, corticospinal tracts, and splenium of the corpus callosum; they also had significantly greater MWF in frontal white matter regions, including the corona radiata, genu of the corpus callosum, and orbitofrontal cortex. The posterior MWF reductions and MWF increases remained significant in the comparison of $\epsilon 4$ carriers and noncarriers younger than 6 months.

6- to 22-Month-Old GMV Comparison

Differences between the 6- to 22-month-old *APOE* $\epsilon 4$ carrier and noncarrier groups in regional GMV are shown in Figure 3 and Table 1. Compared with noncarriers, 6- to 22-month-old $\epsilon 4$ carriers had reduced GMVs in the bilateral precuneus, posterior/middle cingulate, and occipitotemporal and left lateral temporal regions, which are preferentially affected in the later preclinical and clinical stages of AD; they also had greater GMV in medial and lateral frontal regions ($P < .001$, uncorrected for multiple comparisons). Our findings are consistent with some, but not all, of the findings recently reported in 1- to 3-month-old infants.¹⁷

Associations Between Brain Imaging Measurements and Age

As shown in Figure 4, there were highly significant associations ($P < .001$, cluster-corrected for multiple comparisons) between MWF and age in the 2- to 25-month-old $\epsilon 4$ carrier and noncarrier groups. Compared with noncarriers, $\epsilon 4$ carriers had a significantly attenuated relationship between MWF and age (ie, reduced MWF development rate) in extensive white matter locations, including optic radiations, corticospinal tracts, and splenium of the corpus callosum. Compared with noncarriers, $\epsilon 4$ carriers also had significantly stronger relationships between MWF and age in more restricted locations, including frontal and association white matter regions and those that have been previously shown to be associated with *APOE* genotype ($\epsilon 4\epsilon 4$ or $\epsilon 4\epsilon 4 > \epsilon 3\epsilon 3 > \epsilon 2\epsilon 3$) in cognitively unimpaired older adults.³⁶ (As expected, logarithmic and linear models yielded nearly identical relationships between mean MWF and age, but the logarithm model was able to do so with greater statistical power [eg, logarithmic r^2 of 0.86 vs linear r^2 of 0.69 in corpus callosum regions of interest, 0.83 vs 0.76 frontal white matter regions of interest, and 0.84 vs 0.72 in cerebellar white matter regions of interest].) Results from the bootstrap analysis were supported by more conventional log(age) vs group interaction analysis, which provided similar results (not shown).

Of interest, areas showing greater MWF development in the $\epsilon 4$ carriers vs noncarriers were found to lie preferentially along the white matter/gray matter boundaries. A possible reason for this is partial-volume effects within these regions. However, the white matter/gray matter boundary is continuously evolving over this age range, as both white matter and gray matter myelinate, and thus, this finding could relate to myelin development differences within gray matter.

Only 1 location associated with maximally significant GMV differences in the 5- to 22-month-old $\epsilon 4$ carrier and noncarrier groups (Table 1) was found to have a significant association with age in either of the subject groups: GMVs in the left precuneus were inversely associated with age in the noncarriers ($r = -0.58$; $P = .0002$; $P = .002$ after Bonferroni correction), but not in the $\epsilon 4$ carriers ($r = 0.022$, $P = .92$). While the inverse association was greater in the carriers than noncarriers ($P = .02$), this finding did not survive correction for multiple comparisons, could well reflect type I error, and would need to be confirmed in further independent studies.

Discussion

While our findings should be considered preliminary, this study demonstrates some of the earliest brain changes associated with the major genetic risk factor for late-onset AD. Infant $\epsilon 4$ carriers had lower MWF and GMV measurements than noncarriers in the precuneus, posterior/middle cingulate, lateral temporal, and medial occipitotemporal regions, which are preferentially affected by AD, and greater MWF and GMV measurements in frontal regions. The MWF findings remained significant in the subset of 2- to 6-month-old infants. Infant $\epsilon 4$ carriers also exhibited an attenuated relationship between MWF and age in extensive (including earlier developing, posterior) white matter regions and a stronger relationship in more restricted, later developing frontal and associated white matter regions.

As part of a broader effort to characterize regional GMV differences in infant carriers and noncarriers of genetic variants that have been implicated in the predisposition to several psychiatric disorders, Knickmeyer and colleagues¹⁷ recently compared MRIs from 66 *APOE* $\epsilon 4$ carriers and 156 noncarriers 1 to 3 months of age. Many of the infants had a parental psychiatric history and a past parental substance use disorder history, many were monozygotic or dizygotic twins, and a different image-analysis technique was used to compare GMV in the carrier and noncarrier groups. By comparison, our study compared regional GMVs in 6- to 22-month-old singleton infant $\epsilon 4$ carriers and noncarriers without a parental history of psychiatric disorders, neurological disorders, or medication use, it compared a measure of regional white matter myelin content in 2- to 25-month-old carriers and noncarriers, and it investigated their relationship to brain development over these broader age ranges.

In comparison with noncarriers, $\epsilon 4$ carriers in the Knickmeyer et al study had lower GMV in lateral and medial temporal, occipitotemporal, frontal, and precuneus regions and greater GMV in posterior parietal, occipital, middle cingulate, and other frontal and precuneus regions. Some of their $\epsilon 4$ -related findings in the 2 studies are similar (posterior parietotemporal, occipitotemporal, and precuneus locations and frontal increases), other

differences appear to be directly opposing (ie, increases in other precuneus locations in the prior study), and other differences were in reported in only 1 of the 2 studies. Differences in the reported GMV findings could be attributable to differences in infant age, inclusion criteria, image acquisition, or image analysis, limited statistical power, or our decision to restrict the analysis to infants with adequate segmented gray matter images, as noted later. In contrast to the study by Knickmeyer and colleagues, our GMV analysis excluded infants younger than 6 months from the GMV analysis because of the inability of our automated image-analysis algorithm to generate adequate segmented gray matter images in 9 of the 22 infants, including a higher proportion of $\epsilon 4$ carriers than noncarriers. Our mcDESPOT MWF findings suggest that this failure may be related to insufficient myelination in the youngest infants, particularly in those with the $\epsilon 4$ allele. Despite the study differences, the 2 studies provide a foundation for investigating the earliest postnatal neurodevelopmental changes associated with the differential genetic risk for AD and the role of the *APOE* allele on white and gray matter development.

While we cannot exclude the possibility completely, regional GMV differences in the 6- to 25-month-old infants do not seem to be solely attributable to differences in gray matter/white matter contrast (eg, a potential overestimation of GMV of gray matter in locations with less myelination). The automated image-analysis algorithm generated adequately segmented gray matter images in all of the infants in this age group, $\epsilon 4$ -related GMV reductions coincided with white matter MWF reductions (not increases) in posterior regions, and $\epsilon 4$ -related GMV increases coincided with MWF increases (not reductions) in frontal regions.

The *APOE* protein participates in the transport and clearance of cholesterol, which could have effects on the development, maintenance, and repair of synapses and myelinated neurons.³⁷ *APOE* isoforms differ in the extent to which they are expressed ($\epsilon 2 > \epsilon 3 > \epsilon 4$) and folded, perhaps accounting for differential effects on $A\beta$ accumulation and clearance, brain metabolism, tau dephosphorylation, inflammation, neuronal plasticity and repair, other physiological processes, brain development, and the risk of AD. Additional studies are needed to clarify the role of *APOE* in neuronal, synaptic, and myelin development, whether and how *APOE* isoforms may influence these neurodevelopmental processes, and whether and how these neurodevelopmental processes may be relevant to the subsequent development of AD and whether these neurodevelopmental processes are affected by any of the other genetic risk factors for AD.

We have previously postulated that young adults at genetic risk for AD have a reduction in the density, activity, or metabolism of terminal neuronal fields or perisynaptic glial cells in preferentially affected brain regions, that the underlying processes provide a foothold for subsequent pathogenic changes, and that they are developmental.^{6,9,10} Regional GMV reductions in infant $\epsilon 4$ carriers are at least partly consistent with this possibility. The $\epsilon 4$ -related increases in frontal GMV and MWF increases are more difficult to understand at this time.

In an MRI study of healthy older adults, Bartzokis and colleagues³⁶ found that *APOE* variants ($\epsilon 4 > \epsilon 3 > \epsilon 2$) were associated with a steeper rate of myelin breakdown in

latemyelinating frontal regions and that *APOE*-mediated myelin development, maintenance, and repair mechanisms may contribute to the predisposition to AD. Interestingly, our study found that infant $\epsilon 4$ carriers had greater MWF in relatively late-maturing frontal white matter regions, less MWF in relatively early-maturing posterior white matter regions, and an attenuated relationship between MWF and age during the course of infant development. The current study raises new questions about the role of *APOE* in myelin development, the influence of *APOE* variants on this process, and the extent to which myelin development contributes to the predisposition to AD.

Studies have not yet resolved whether cognitive impairment is slightly better, slightly worse, or completely unaffected in infants, children, adolescents, and young adults with and without the *APOE* $\epsilon 4$ allele. According to a recent meta-analysis of studies in children, adolescents, and young adults, Ihle and colleagues³⁸ reported the following. Several small studies (as well as a small study assessing mental development in 24-month-old infants³⁹) have suggested slightly better cognitive performance than noncarriers in $\epsilon 4$ carriers, particularly on executive tasks, leading to the idea that better executive performance and greater frontal cortex activation during associative memory tasks reflects compensatory processes. Other small studies have suggested slightly worse cognitive performance in $\epsilon 4$ carriers. Large studies have failed to detect differences between carriers and noncarriers in their executive or other cognitive task performance, IQ, or educational attainment, and their meta-analysis of 20 studies involving more than 11 000 nine-to 31-year-old $\epsilon 4$ carriers and noncarriers failed to support a significant difference in executive or overall cognitive performance. Our findings underscore the need for larger cross-sectional and longitudinal studies to characterize and compare performance on executive and other cognitive domains starting in infancy.

An open question, however, remains as to the benefit of increased myelin content or faster myelin development rate at these young ages. While scant evidence exists to suggest increased myelin content directly benefits cognitive or behavioral processing, there is strong evidence for a strong spatiotemporal association between white matter myelination and behavioral maturation and that delayed myelination is associated with developmental delay.^{40,41}

This study has several limitations. Since the reported regional GMV changes did not survive statistical correction for multiple comparisons, these findings should be considered exploratory and need to be confirmed in subsequent studies. Still, the uncorrected *P* values exceeded a threshold ($P < .001$) that we have consistently found to optimize the trade-off between type I and type II error (because of the smaller number of independent comparisons in connected brain regions), the implicated voxel clusters were extensive and bilateral, some of the *P* values approached $P = .00001$, and some of the $\epsilon 4$ -related regional GMV differences were reported in the prior infant MRI study. While cross-sectional analyses permitted us to characterize and compare associations between brain imaging measurements and age in the carrier and noncarrier groups, longitudinal studies are needed to characterize and compare trajectories with greater statistical power. Additional studies are needed to clarify the extent to which our $\epsilon 4$ - and age-related findings are attributable to differences in gray matter/white matter contrast.

Conclusions

Findings from this study raise new questions about the role of *APOE* in normal human brain development and the earliest processes involved in the predisposition to AD, their possible relationship to subsequent AD pathology, and the extent to which they can be targeted by AD prevention therapies.

Acknowledgments

Funding/Support: Funding for this study was provided by National Institutes of Mental Health grant R01 MH087510 (Dr Deoni), National Institute on Aging grants R01 AG031581 (Dr Reiman) and P30 AG19610 (Dr Reiman), the state of Arizona (Dr Reiman), Department of Defense, Air Force Office of Scientific Research National Defense Science and Engineering Graduate Fellowship 32 CFR 168a (Dr Madsen), and Sir Henry Wellcome Postdoctoral Fellowship 096195 (Dr O’Muircheartaigh).

Role of the Sponsor: The funders had no role in the design and conduct of the study; collection, management, analysis, and interpretation of the data; and preparation, review, or approval of the manuscript; and decision to submit the manuscript for publication.

REFERENCES

1. Hardy JA, Higgins GA. Alzheimer’s disease: the amyloid cascade hypothesis. *Science*. 1992; 256(5054):184–185. [PubMed: 1566067]
2. Reitz C. Alzheimer’s disease and the amyloid cascade hypothesis: a critical review. *Int J Alzheimers Dis*. 2012; 2012:369808. [PubMed: 22506132]
3. Bateman RJ, Xiong C, Benzinger TL, et al. Dominantly Inherited Alzheimer Network. Clinical and biomarker changes in dominantly inherited Alzheimer’s disease. *N Engl J Med*. 2012; 367(9):795–804. [PubMed: 22784036]
4. Jack CR Jr, Knopman DS, Jagust WJ, et al. Hypothetical model of dynamic biomarkers of the Alzheimer’s pathological cascade. *Lancet Neurol*. 2010; 9(1):119–128. [PubMed: 20083042]
5. Price JL, Morris JC. Tangles and plaques in nondemented aging and “preclinical” Alzheimer’s disease. *Ann Neurol*. 1999; 45(3):358–368. [PubMed: 10072051]
6. Bookheimer SY, Strojwas MH, Cohen MS, et al. Patterns of brain activation in people at risk for Alzheimer’s disease. *N Engl J Med*. 2000; 343(7):450–456. [PubMed: 10944562]
7. Shaw P, Lerch JP, Pruessner JC, et al. Cortical morphology in children and adolescents with different apolipoprotein E gene polymorphisms: an observational study. *Lancet Neurol*. 2007; 6(6): 494–500. [PubMed: 17509484]
8. Sheline YI, Morris JC, Snyder AZ, et al. APOE4 allele disrupts resting state fMRI connectivity in the absence of amyloid plaques or decreased CSF A β 42. *J Neurosci*. 2010; 30(50):17035–17040. [PubMed: 21159973]
9. Crivello F, Lemaître H, Dufouil C, et al. Effects of ApoE-epsilon4 allele load and age on the rates of grey matter and hippocampal volumes loss in a longitudinal cohort of 1186 healthy elderly persons. *Neuroimage*. 2010; 53(3):1064–1069. [PubMed: 20060049]
10. Ewers M, Sperling RA, Klunk WE, Weiner MW, Hampel H. Neuroimaging markers for the prediction and early diagnosis of Alzheimer’s disease dementia. *Trends Neurosci*. 2011; 34(8): 430–442. [PubMed: 21696834]
11. Mahley RW, Rall SC Jr. Apolipoprotein E: far more than a lipid transport protein. *Annu Rev Genomics Hum Genet*. 2000; 1:507–537. [PubMed: 11701639]
12. Corder EH, Saunders AM, Strittmatter WJ, et al. Gene dose of apolipoprotein E type 4 allele and the risk of Alzheimer’s disease in late onset families. *Science*. 1993; 261(5123):921–923. [PubMed: 8346443]
13. Strittmatter WJ, Roses AD. Apolipoprotein E and Alzheimer disease. *Proc Natl Acad Sci U S A*. 1995; 92(11):4725–4727. [PubMed: 7761390]

14. Filippini N, MacIntosh BJ, Hough MG, et al. Distinct patterns of brain activity in young carriers of the APOE-epsilon4 allele. *Proc Natl Acad Sci U S A*. 2009; 106(17):7209–7214. [PubMed: 19357304]
15. Buckner RL, Snyder AZ, Sanders AL, Raichle ME, Morris JC. Functional brain imaging of young, nondemented, and demented older adults. *J Cogn Neurosci*. 2000; 12(suppl 2):24–34. [PubMed: 11506645]
16. He Y, Wang L, Zang Y, et al. Regional coherence changes in the early stages of Alzheimer's disease: a combined structural and resting-state functional MRI study. *Neuroimage*. 2007; 35(2): 488–500. [PubMed: 17254803]
17. Knickmeyer RC, Wang J, Zhu H, et al. Common variants in psychiatric risk genes predict brain structure at birth. *Cereb Cortex*. 2014; 24:1230–1246. doi:10.1176/appi.pn.2013.2a13. [PubMed: 23283688]
18. Deoni SCL, Dean DC III, O'Muirheartaigh J, Dirks H, Jerskey BA. Investigating white matter development in infancy and early childhood using myelin water fraction and relaxation time mapping. *Neuroimage*. 2012; 63(3):1038–1053. [PubMed: 22884937]
19. Deoni SCL, Mercure E, Blasi A, et al. Mapping infant brain myelination with magnetic resonance imaging. *J Neurosci*. 2011; 31(2):784–791. [PubMed: 21228187]
20. Kitzler HH, Su J, Zeineh M, et al. Deficient MWF mapping in multiple sclerosis using 3D whole-brain multi-component relaxation MRI. *Neuroimage*. 2012; 59(3):2670–2677. [PubMed: 21920444]
21. Kolind S, Matthews L, Johansen-Berg H, et al. Myelin water imaging reflects clinical variability in multiple sclerosis. *Neuroimage*. 2012; 60(1):263–270. [PubMed: 22155325]
22. Yakovlev, PI.; Lecours, AR. The myelogenetic cycles of regional maturation of the brain. In: Minkowski, A., editor. *Regional Development of the Brain in Early Life*. Blackwell Scientific Publications; Oxford, England: 1967.
23. Hurley, SA.; Mossahebi, PM.; Samsonov, AA., et al. Proceedings of the 18th Annual Meeting of the ISMRM, Stockholm, Sweden. ISMRM; Stockholm, Sweden: 2010. Multicomponent relaxometry (mcDESPOT) in the Shaking Pup Model of Dysmyelination; p. 4516
24. MacKay A, Laule C, Vavasour I, Bjarnason T, Kolind S, Mädler B. Insights into brain microstructure from the T2 distribution. *Magn Reson Imaging*. 2006; 24(4):515–525. [PubMed: 16677958]
25. Deoni SCL, Matthews L, Kolind SH. One component? Two components? Three? The effect of including a nonexchanging “free” water component in multicomponent driven equilibrium single pulse observation of T1 and T2. *Magn Reson Med*. 2013; 70(1):147–154. [PubMed: 22915316]
26. Laule C, Leung E, Lis DK, et al. Myelin water imaging in multiple sclerosis: quantitative correlations with histopathology. *Mult Scler*. 2006; 12(6):747–753. [PubMed: 17263002]
27. Webb S, Munro CA, Midha R, Stanisz GJ. Is multicomponent T2 a good measure of myelin content in peripheral nerve? *Magn Reson Med*. 2003; 49(4):638–645. [PubMed: 12652534]
28. Avants BB, Epstein CL, Grossman M, Gee JC. Symmetric diffeomorphic image registration with cross-correlation: evaluating automated labeling of elderly and neurodegenerative brain. *Med Image Anal*. 2008; 12(1):26–41. [PubMed: 17659998]
29. Jenkinson M, Bannister PR, Brady M, Smith S. Improved optimization for the robust and accurate linear registration and motion correction of brain images. *Neuroimage*. 2002; 17(2):825–841. [PubMed: 12377157]
30. Smith SM. Fast robust automated brain extraction. *Hum Brain Mapp*. 2002; 17(3):143–155. [PubMed: 12391568]
31. Deoni SCL. Correction of main and transmit magnetic field (B0 and B1) inhomogeneity effects in multicomponent-driven equilibrium single-pulse observation of T1 and T2. *Magn Reson Med*. 2011; 65(4):1021–1035. [PubMed: 21413066]
32. Worsley KJ, Andermann M, Koullis T, MacDonald D, Evans AC. Detecting changes in nonisotropic images. *Hum Brain Mapp*. 1999; 8(2-3):98–101. [PubMed: 10524599]
33. Altaye M, Holland SK, Wilke M, Gaser C. Infant brain probability templates for MRI segmentation and normalization. *Neuroimage*. 2008; 43(4):721–730. [PubMed: 18761410]

34. Efron B. Bootstrap methods: another look at the jackknife. *Ann Stat.* 1979; 7(1):1–26. doi: 10.1214/aos/1176344552.
35. Miller, DC. *Handbook of Research Design and Social Measurement*. David McKay Company Inc; New York, NY: 1977.
36. Bartzokis G, Lu PH, Geschwind DH, Edwards N, Mintz J, Cummings JL. Apolipoprotein E genotype and age-related myelin breakdown in healthy individuals: implications for cognitive decline and dementia. *Arch Gen Psychiatry.* 2006; 63(1):63–72. [PubMed: 16389198]
37. Hauser PS, Narayanaswami V, Ryan RO. Apolipoprotein E: from lipid transport to neurobiology. *Prog Lipid Res.* 2011; 50(1):62–74. [PubMed: 20854843]
38. Ihle A, Bunce D, Kliegel M. APOE ϵ 4 and cognitive function in early life: a meta-analysis. *Neuropsychology.* 2012; 26(3):267–277. [PubMed: 22329498]
39. Wright RO, Hu H, Silverman EK, et al. Apolipoprotein E genotype predicts 24-month Bayley Scales infant development score. *Pediatr Res.* 2003; 54(6):819–825. [PubMed: 12930912]
40. Pujol J, López-Sala A, Sebastián-Gallés N, et al. Delayed myelination in children with developmental delay detected by volumetric MRI. *Neuroimage.* 2004; 22(2):897–903. [PubMed: 15193620]
41. Nagy Z, Westerberg H, Klingberg T. Maturation of white matter is associated with the development of cognitive functions during childhood. *J Cogn Neurosci.* 2004; 16(7):1227–1233. [PubMed: 15453975]

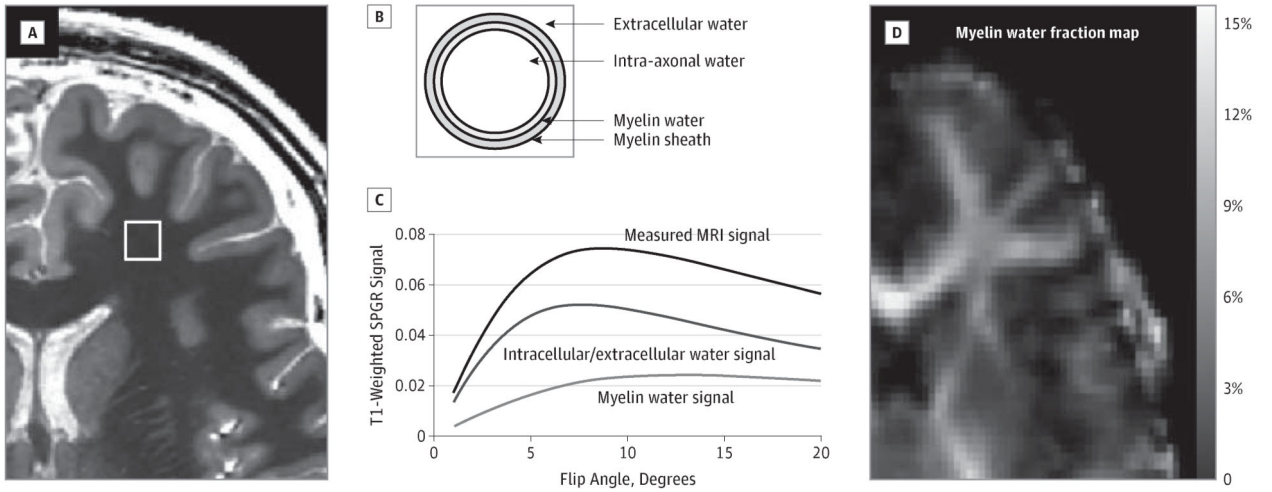


Figure 1. Derivation of MWF Estimates

Each voxel within the image (A) is assumed to comprise water trapped within the lipid bilayers of the myelin sheath in chemical exchange with intracellular and extracellular water (B), as well as a third nonexchanging “free” water compartment attributable to cerebral spinal fluid. mcDESPOT (multi-component Driven Equilibrium Single Pulse Observation of T1 and T2) processing fits a mathematical form of this tissue model to the acquired data (C) to derive the relaxation times and volume fractions of each compartment. The volume fraction of the myelin water is termed the *myelin water fraction* (D). MRI indicates magnetic resonance imaging and SPGR, spoiled gradient recalled echo images.

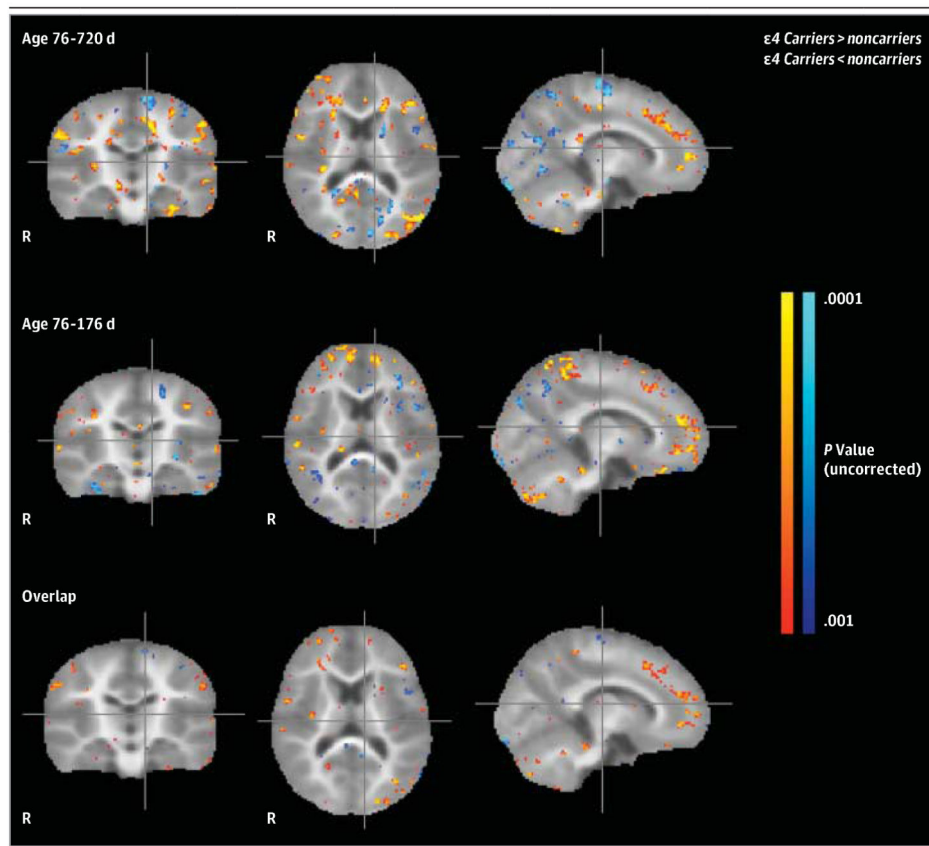


Figure 2. Differences Between Infant Apolipoprotein E $\epsilon 4$ Carriers and Noncarriers in Regional Myelin Water Fraction (MWF), a Measure of White Matter Myelin Content

First row: Between-group MWF differences using data from the entire cohort of 2- to 25-month-old infants. Second row: Between-group MWF differences using data from the subset of infants younger than 6 months. Third row: Overlap of regional MWF differences observed in initial and subset analyses. Compared with their respective noncarrier groups, the 2- to 26-month-old and 2- to 6-month-old $\epsilon 4$ carrier groups had reduced MWFs in white matter regions that mature earlier, including optic radiations, corticospinal tracts, and splenium of the corpus callosum, and increased MWF in frontal white matter regions that mature later, including frontal white matter, the corona radiata, and genu of the corpus callosum ($P < .001$, uncorrected for multiple comparisons). The magnitude and atlas locations of maximally significant differences in regional MWF are shown in Table 1.

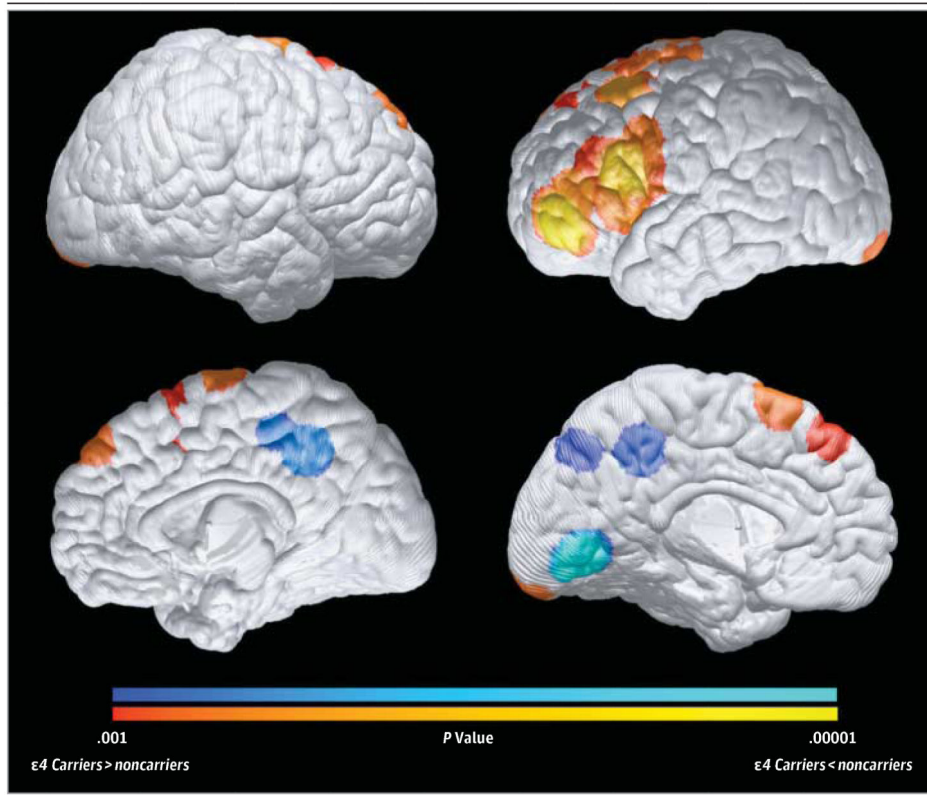


Figure 3. Differences Between Infant Apolipoprotein E $\epsilon 4$ Carriers and Noncarriers in Regional Gray Matter Volumes (GMVs)

Compared with noncarriers, 6- to 22-month-old $\epsilon 4$ carriers had significantly reduced GMVs in the bilateral precuneus, posterior/middle cingulate, and occipitotemporal regions (as shown in blue) and in a left lateral temporal region (not shown, because it is too deep to be projected onto the cortical surface), which are preferentially affected in the later preclinical and clinical stages of Alzheimer disease, and significantly greater GMVs (in red) in bilateral medial and lateral frontal regions ($P < .001$, uncorrected for multiple comparisons). Statistical maps are projected onto the medial and lateral surfaces of a spatially standardized 12-month-old infant's brain. The magnitude and atlas locations of maximally significant differences in regional GMV are shown in Table 1.

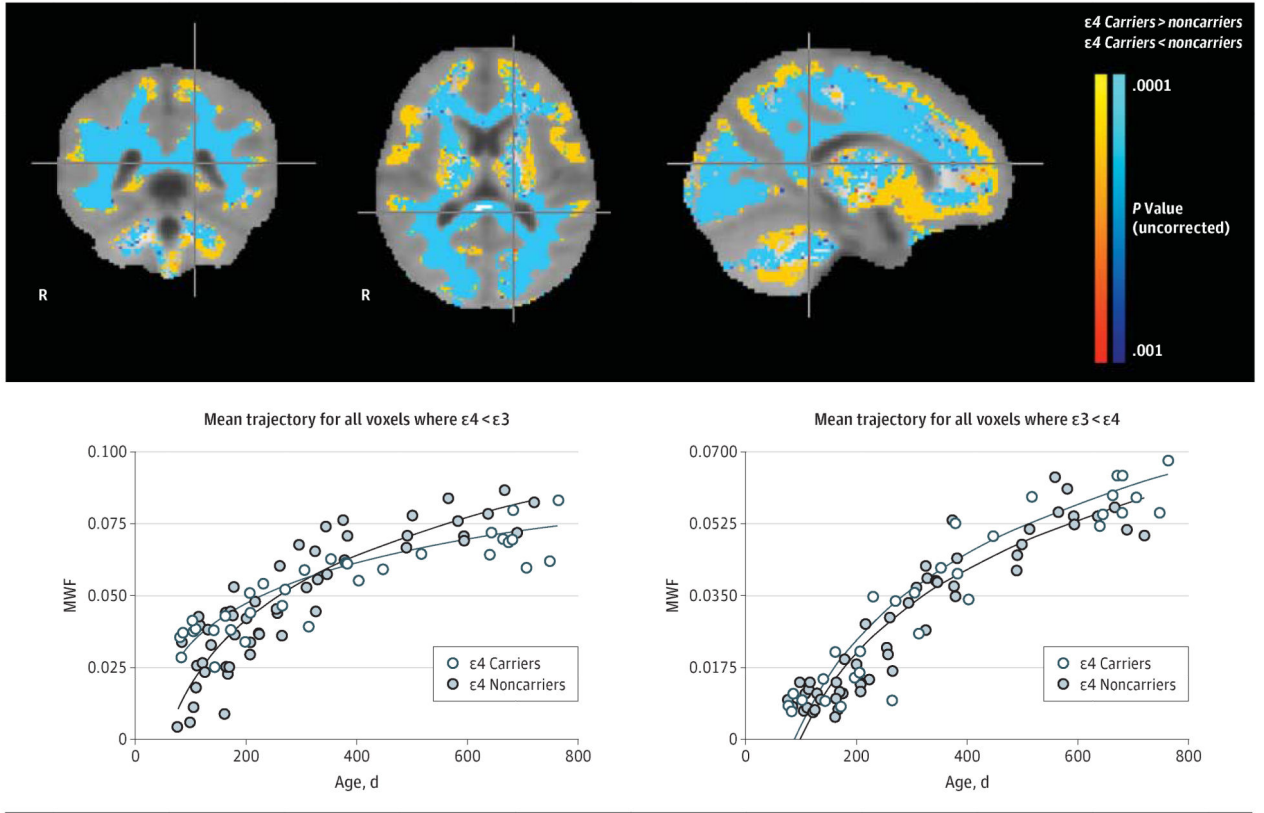


Figure 4. Associations Between Myelin Water Fraction (MWF) and Age in the Infant Apolipoprotein E ε4 Carrier and Noncarrier Groups

Top: Regions in which the associations between MWF, a measure of myelin content, and age are significantly different in the 2- to 25-month-old ε4 carrier and noncarrier groups. The extensive white matter regions with a significantly attenuated association between MWF and age in the ε4 carrier group are shown in blue; they include optic radiations, corticospinal tracts, and splenium of the corpus callosum, which are known to mature in the earlier stages of brain development. The more limited white matter regions with a significantly stronger association between MWF and age in the ε4 carrier group are shown in orange; they include frontal and associated white matter regions that are known to mature in the later stages of brain development. Bottom: Mean age-related MWF trajectories and their corresponding bootstrap resampling distributions in the 2- to 25-month-old ε4 carrier and noncarrier groups are shown for whole-brain white matter, left optic radiation, and genu of corpus callosum regions of interest. Associations between MWF and age in these regions of interest were significantly attenuated in the ε4 carrier group.

Table 1
Location and Magnitude of Most Significant Differences Between Infant Apolipoprotein E ϵ 4 Carriers and Noncarriers in Regional Myelin Water Fraction (MWF) and Gray Matter Volume (GMV)

Region	↓ or ↑	Atlas Coordinate ^a			P Value ^b
		x	y	z	
Locations with altered MWF in ϵ 4 carriers (aged 76-176 d)					
Frontal	↑	9	43	16	.00002 ^c
Frontal	↑	-12	42	16	.00002 ^c
Parietal	↑	20	-42	60	.00032
Parietal	↑	-9	-42	56	.00001 ^c
Cerebellum	↑	-18	-66	-24	.0008
Corticospinal tract	↓	-18	-17	53	.0003 ^c
Locations with altered MWF in ϵ 4 carriers (aged 76-720 d)					
Superior corona radiata	↑	24	8	30	.00001 ^c
Superior corona radiata	↑	-18	10	30	.00002 ^c
Inferior fronto-occipital fasciculus	↑	33	30	10	.0003 ^c
Genu of the corpus callosum	↑	60	18	11	.0005 ^c
Corticospinal tract	↓	11	-28	58	.003
Corticospinal tract	↓	-14	-23	58	.0004 ^c
Optic radiation	↓	-17	-59	17	.002
Locations with altered GMV in ϵ 4 carriers					
Precuneus and precuneus/cingulate	↓	-8	-70	40	.0009
Precuneus	↓	2	-43	39	.0005
Precuneus/cingulate	↓	-38	-50	17	.00005
Medial occipitotemporal*	↓	-4	-72	-3	.00008
Frontal	↑	-10	20	58	.0004
Supplemental motor area	↑	12	16	54	.001
Midfrontal	↑	-30	22	43	.0002
Inferior frontal gyrus (triangularis)	↑	-57	18	14	.00002
Inferior frontal gyrus (triangularis)	↑	30	4	44	.0008
Middle orbital frontal gyrus	↑	-46	46	-9	.00001

Abbreviations: ↓, decreased; ↑, increased.

^aCoordinates from the Talairach brain atlas, such that x is the distance in millimeters to the right (+) or left (-) of midline, y is the distance anterior (+) or posterior (-) to the anterior commissure, and z is the distance above (+) or below (-) a horizontal plane through the anterior and posterior commissures.

^bP values, uncorrected for multiple comparisons.

^cFindings that remained significant after correcting for multiple regional comparisons using cluster-based correction with a clusterthreshold of 2.5.

Table 2
Characteristics of the Infant Apolipoprotein E $\epsilon 4$ Carrier and Noncarrier Groups^a

	Mean (SD)		P Value ^b
	$\epsilon 4$ Carriers	$\epsilon 4$ Noncarriers	
2- to 25-month-old infant regional MWF comparison			
No. of participants	60	102	
Genotype, No.	6 $\epsilon 4\epsilon 4$, 51 $\epsilon 3\epsilon 4$, 3 $\epsilon 2\epsilon 4$	86 $\epsilon 3\epsilon 3$, 16 $\epsilon 2\epsilon 3$, 0 $\epsilon 2\epsilon 2$	
Age, d	391 (196)	366 (181)	.36
Gestation, wk	39.8 (1.5)	39.6 (1.9)	.46
Female/male	25/35	54/48	.28
Maternal age, y	29.6 (6.1)	29.7 (5.2)	.89
Maternal SES ^c	5.7 (0.9)	5.7(1.1)	.76
2- to 6-month-old infant regional MWF comparison			
No. of participants	14	22	
Genotype, No.	2 $\epsilon 4\epsilon 4$, 9 $\epsilon 3\epsilon 4$, 3 $\epsilon 2\epsilon 4$	16 $\epsilon 3\epsilon 3$, 6 $\epsilon 2\epsilon 3$, 0 $\epsilon 2\epsilon 2$	
Age, d	118 (32)	127(33)	.44
Gestation, wk	39.2 (1.2)	39.3 (1.3)	.49
Female/male	8/6	12/10	.49
Maternal age, y	32.1 (4.1)	30.2 (4.1)	.31
Maternal SES ^c	6(1)	5.4(1.2)	.32
6- to 22-month-old infant regional GMV comparison			
No. of participants	23	36	
Genotype, No.	3 $\epsilon 4\epsilon 4$, 17 $\epsilon 3\epsilon 4$, 3 $\epsilon 2\epsilon 4$	29 $\epsilon 3\epsilon 3$, 7 $\epsilon 2\epsilon 3$, 0 $\epsilon 2\epsilon 2$	
Age, d	399 (123)	414 (141)	.66
Gestation, wk	39.5 (1.2)	39.2 (1.3)	.35
Female/male	11/12	20/16	.60
Maternal age, y	30.1 (5.2)	29.4 (5.9)	.66
Maternal SES ^c	5.8 (1.2)	5.5 (0.9)	.38

Abbreviations: GMV, gray matter volume; MWF, myelin water fraction; SES, socioeconomic status.

^a Infant ages were corrected to an estimated 40-week gestational duration.

^b Groups were compared for gestational age, maternal age, and maternal SES using a 2-sample *t* test and for sex differences, using a χ^2 test.

^c Maternal SES was evaluated using the Hollingshead Two-Factor Index of Social Position.³⁵

Table 3
Additional Demographic Features of the Infant Apolipoprotein E ϵ 4 Carrier and Noncarrier Groups

	No. of Participants		P Value ^a
	ϵ 4 Carriers	ϵ 4 Noncarriers	
2- to 25-month-old infant regional MWF comparison			
No. of participants	60	102	
Child feeding (breast/bottle/both)	23/16/21	42/21/39	.17
In utero smoke exposure (exposed/not exposed)	5/55	7/95	.84
Birth type (vaginal/cesarean)	44/16	77/25	.77
Marital status (married or living together/divorced or single)	52/8	77/25	.55
Maternal education level, mean (SD) ^b	5.01	5.16	.31
2- to 6-month-old infant regional MWF comparison			
No. of participants	14	22	
Child feeding (breast/bottle/both)	5/6/3	7/5/10	.27
In utero smoke exposure (exposed/not exposed)	0/14	2/22	.16
Birth type (vaginal/cesarean)	10/4	18/4	.68
Marital status (married or living together/divorced or single)	10/4	19/3	.49
Maternal education level, mean (SD) ^b	5.5	5.4	.42
6- to 22-month-old infant regional GMV comparison			
No. of participants	23	36	
Child feeding (breast/bottle/both)	8/7/8	9/10/17	.56
In utero smoke exposure (exposed/not exposed)	5/18	5/31	.19
Birth type (vaginal/cesarean)	19/4	26/10	.52
Marital status (married or living together/divorced or single)	18/5	27/9	.91
Maternal education level, mean (SD) ^b	4.95	5.03	.16

Abbreviations: GMV, gray matter volume; MWF, myelin water fraction.

^a All groups were compared using a χ^2 test.

^b Maternal education level was evaluated using the Education Scale of the Hollingshead Two-Factor Index of Social Position.³⁵